Comparison of Thermal Management Approaches for Integrated Traction Drives in Electric Vehicles

Preprint

Bidzina Kekelia,[1] J. Emily Cousineau,[1] Kevin Bennion,[1] Sreekant Narumanchi,[1] and Shajjad Chowdhury[2]

1 National Renewable Energy Laboratory
2 Oak Ridge National Laboratory

Presented at the ASME 2020 International Technical Conference and Exhibition on Packaging and Integration of Electronic and Photonic Microsystems (InterPACK2020)
October 27-29, 2020

NREL is a national laboratory of the U.S. Department of Energy
Office of Energy Efficiency & Renewable Energy
Operated by the Alliance for Sustainable Energy, LLC

This report is available at no cost from the National Renewable Energy Laboratory (NREL) at www.nrel.gov/publications.

Contract No. DE-AC36-08GO28308

Conference Paper
NREL/CP-5400-77160
October 2020

Comparison of Thermal Management Approaches for Integrated Traction Drives in Electric Vehicles

Preprint

Bidzina Kekelia,[1] J. Emily Cousineau,[1] Kevin Bennion,[1] Sreekant Narumanchi,[1] and Shajjad Chowdhury[2]

1 National Renewable Energy Laboratory
2 Oak Ridge National Laboratory

Suggested Citation
Kekelia, Bidzina, J. Emily Cousineau, Kevin Bennion, Sreekant Narumanchi, and Shajjad Chowdhury. 2020. *Comparison of Thermal Management Approaches for Integrated Traction Drives in Electric Vehicles: Preprint*. Golden, CO: National Renewable Energy Laboratory. NREL/CP-5400-77160. https://www.nrel.gov/docs/fy21osti/77160.pdf.

NREL is a national laboratory of the U.S. Department of Energy
Office of Energy Efficiency & Renewable Energy
Operated by the Alliance for Sustainable Energy, LLC

This report is available at no cost from the National Renewable Energy Laboratory (NREL) at www.nrel.gov/publications.

Contract No. DE-AC36-08GO28308

Conference Paper
NREL/CP-5400-77160
October 2020

National Renewable Energy Laboratory
15013 Denver West Parkway
Golden, CO 80401
303-275-3000 • www.nrel.gov

NOTICE

This work was authored in part by the National Renewable Energy Laboratory, operated by Alliance for Sustainable Energy, LLC, for the U.S. Department of Energy (DOE) under Contract No. DE-AC36-08GO28308. Funding provided by U.S. Department of Energy Office of Energy Efficiency and Renewable Energy Vehicle Technologies Office. The views expressed herein do not necessarily represent the views of the DOE or the U.S. Government. The U.S. Government retains and the publisher, by accepting the article for publication, acknowledges that the U.S. Government retains a nonexclusive, paid-up, irrevocable, worldwide license to publish or reproduce the published form of this work, or allow others to do so, for U.S. Government purposes.

Cover Photos by Dennis Schroeder: (clockwise, left to right) NREL 51934, NREL 45897, NREL 42160, NREL 45891, NREL 48097, NREL 46526.

COMPARISON OF THERMAL MANAGEMENT APPROACHES FOR INTEGRATED TRACTION DRIVES IN ELECTRIC VEHICLES

Bidzina Kekelia[1], **J. Emily Cousineau, Kevin Bennion, Sreekant Narumanchi**
National Renewable Energy Laboratory,
Golden, CO, USA

Shajjad Chowdhury
Oak Ridge National Laboratory,
Oak Ridge, TN, USA

ABSTRACT

The continuous push to increase power densities of electric vehicle (EV) traction drive systems necessitates combining electric motor and power electronics into one unit. A single, compact traction drive unit with fewer interconnecting components also facilitates fast, automated assembly of electric vehicles, driving production costs down and enabling wider adoption of EVs. There are a number of challenges associated with the integration of power electronics with the electric machine, including thermal management of the combined traction drive system. However, one important benefit of integration from the thermal management system perspective is the potential for using a single fluid loop instead of two separate cooling systems for the electric machine and the power electronics/inverter.

This paper reviews several integration approaches and, employing finite element analysis (FEA), compares thermal management solutions for the combined electric machine and power electronics systems. Namely, three different scenarios are modeled: (1) independent component (motor and power electronics) cooling, which is compared to the combined cooling system approach for (2) radially and (3) axially integrated power electronics modules into the motor enclosure. Temperature distributions for selected thermal loads and thermal resistances from the key heat-generating components to the cooling fluid are compared for each scenario.

NOMENCLATURE

h	heat transfer coefficient
k	thermal conductivity
Q	dissipated heat due to losses
T_{fluid}	fluid/coolant temperature
T_c	case temperature
T_j	junction layer temperature
I_{DS}	drain to source current
R_{DS}	drain to source resistance
V_{DS}	drain to source voltage

INTRODUCTION

The share of vehicles with fully electric propulsion systems is constantly increasing, and so is their traction drive power. With increasing power and power density of electric traction drives, their thermal management is becoming increasingly challenging. Appropriate thermal design is as important as electromagnetic and mechanical design of the electric machine [1]. In addition to optimizing the passive thermal design (geometric layout of components, material selection, and thermal interfaces affecting the heat-spreading capabilities within the electric motor), it is necessary to actively remove heat from key components of the drive. Cooling of the electric drive in a vehicle can be accomplished by circulating coolant, such as water-ethylene glycol (WEG) or oil, through the stator case or internal passages in the motor, removing heat from the components. Another effective method for cooling an electric motor is impingement of automatic transmission fluid (ATF) jets directly on components (windings) where heat is generated. This technique avoids the conduction path thermal resistance through the passive stack of other materials present in a water jacket WEG-cooling scenario [2]. The heat is ultimately rejected to the ambient air.

The current trend of reducing volume and weight of traction drives to achieve higher power densities leads to integration of a number of propulsion components into a single unit. Integration of power electronics into electric motor casing further complicates thermal management of the traction drive. Two main heat-generation sources in electric vehicle (apart from batteries), often with different cooling requirements and heat removal strategies, are combined into a common space. Thus, without effective thermal management solutions, it is impossible for high-performance, compact (power-dense), and reliable integrated electric traction drives to achieve the 2025 U.S. DRIVE (Driving Research and Innovation for Vehicle efficiency and Energy sustainability) system power-density target of 33 kW/L [3].

This paper provides an overview of the main trends in the integration of electric vehicle propulsion systems and their

[1] Contact author: bidzina.kekelia@nrel.gov

thermal management solutions. Three different topologies are evaluated in the following sections, and their respective thermal management approaches are compared.

MODELING SETUP AND PROCEDURES

Integration trends

Based on research of publicly accessible scientific literature, published automotive original equipment manufacturer (OEM) materials, and interactions with other research groups, three main topologies were identified for integrated electric traction drives currently available in the market or for future trends in their design (see Figure 1), namely:

(1) Power electronics (PE) enclosure attached to electric motor case, eliminating wire harness, but with separate cooling loops [4,5],
(2) PE radially integrated into the electric motor case with shared cooling loop [6,7],
(3) PE axially integrated into the front/back of the electric motor case [8,9].

Each of the above-mentioned approaches is implemented with some degree of variation by different manufacturers or research/design teams. Additional overview and integration enabling technologies are reviewed in [10].

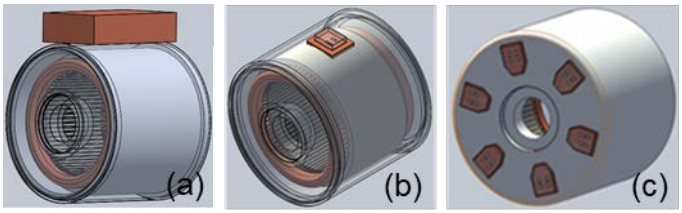

Figure 1. Identified integration concepts: (a) separate PE enclosure attached to motor case, (b) PE distributed/mounted radially on the motor casing, and (c) PE integrated axially in the motor front/back plate.

Computer-aided design (CAD) models

Based on the identified integration trends, simplified CAD models of the integrated traction drive were created. For the electric machine geometry, the 2016 BMW i3 electric traction motor was used. The selection was based on access to its geometry/materials due to the previous teardown/evaluation by Oak Ridge National Laboratory (ORNL) and availability of its detailed benchmarking/losses data [11,12]. The motor losses were used as thermal loads for thermal simulations. The power electronics CAD model was based on newer silicon-carbide (SiC) metal–oxide–semiconductor field-effect transistor (MOSFET) dies from Wolfspeed/Cree (CPM3-0900-0010A). These SiC power devices were previously used by ORNL for modeling a simulated control of the BMW i3 motor with a six-phase power module. Thus, their estimated losses/thermal loads were also available (see discussion in the next section and [13]).

Figure 2 and Figure 3 show radially and axially integrated CAD models, respectively, of an integrated traction drive. For computational efficiency and due to symmetry (PE modules are assumed to be evenly distributed on the outer casing of the motor), only one-sixth of the drive was simulated in the following finite element analysis (FEA) simulations.

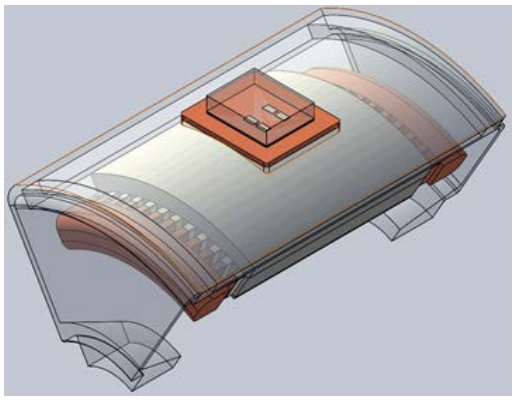

Figure 2. Radially integrated CAD model based on the BMW i3 traction motor and SiC power devices (shared cooling jacket): one-phase power module with one-sixth of the motor.

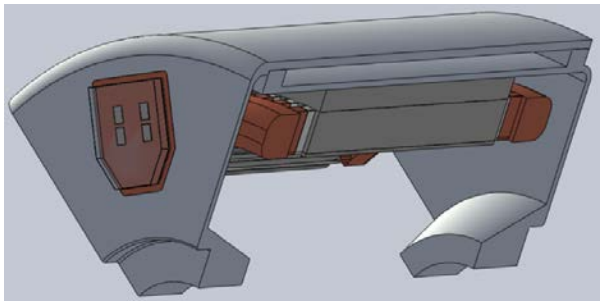

Figure 3. Axially integrated CAD model based on the BMW i3 traction motor and SiC power devices: one-phase power module with one-sixth of the motor.

FEA thermal models

Based on CAD models discussed in the previous section, thermal models were developed for FEA simulations in ANSYS. For the integration approach (1) with separate enclosures and cooling loops for the power electronics and the electric motor, simulations in ANSYS were carried out separately for the power module and the electric motor. For the (2) radially and (3) axially integrated power electronics concepts, thermal models were based on the CAD models shown in Figure 2 and Figure 3, respectively.

FEA thermal simulations in ANSYS were carried out using thermal loads based on ORNL's experimentally measured loss data for the BMW i3 traction motor and estimated inverter losses using a segmented drive-based topology. The segmented drive was realized by dividing the three-phase motor into two sets of three-phase winding (Figure 4). A six-phase inverter was designed to supply these two three-phase motors. A triangular sine carrier-based pulse-width modulation (PWM) technique was used to control the converter where two 90° phase-shifted

carriers were used to reduce DC bus capacitor current stress [14]. A circuit diagram of the drive system is shown in Figure 4.

A SiC-based power module was designed to drive the modified BMW i3 motor and to estimate inverter loss. The designed power module corresponds to one single-phase leg of the inverter, considering two parallel devices to handle the required current. The losses of the designed inverter were estimated with Cree 900V SiC devices using datasheet values and the parameters shown in Table 1. The inverter losses, shown in Figure 5, were estimated using analytical equations developed in [13]. It can be seen that the inverter loss is highest around the knee point of the torque-speed curve due to high torque operation in that area. The experimentally obtained motor losses are shown in Figure 6. These losses are measured at the winding temperature of approximately 105°C.

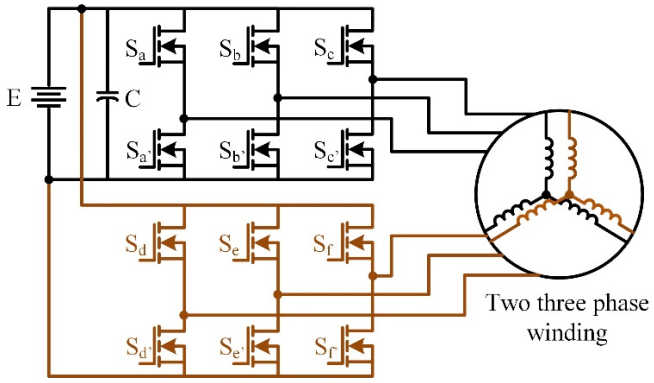

Figure 4. Circuit diagram of a segmented drive.

Table 1. Device and Power Module Parameters

SiC Power Device Datasheet Parameters	
Device	CPM3-0900-0010A
Blocking voltage, V_{DS}	900 V
R_{DS} @ T_j = 170°C	15.4 mΩ
I_{DS} @ T_c = 100°C	140 Arms
Designed Power Module Parameters	
Current handling capacity	280 Arms
Parallel devices	2
Operating DC voltage	360 V

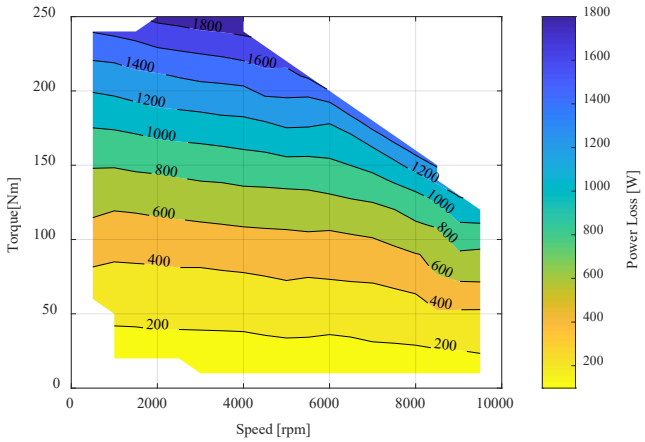

Figure 5. Estimated inverter losses using a simulation platform.

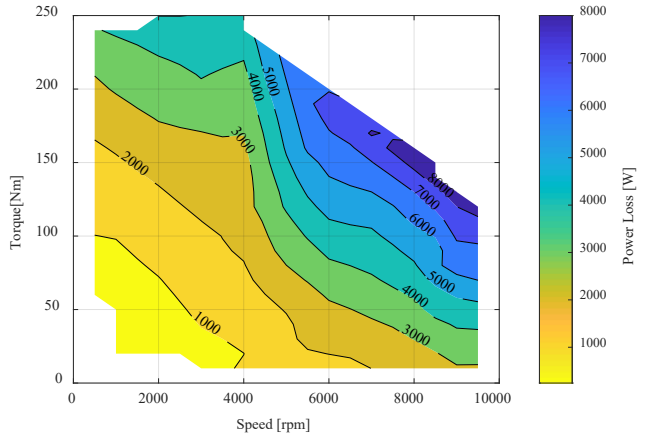

Figure 6. Experimentally obtained BMW i3 motor losses.

The loss values at 11,000 rpm for the BMW i3 traction motor (beyond rpm values shown in Figure 6) and estimated maximum inverter losses of Q = 1,770 W / 6 (six phases with four SiC devices per phase) = 295 W/phase or 73.75 W/device, are utilized in the following sections to estimate the required cooling performance of integrated motor drives. Thermal loads were distributed in the motor components as internal heat generation in the windings, stator yoke, shoe, and teeth. For the power module, the heat flow was applied to the top surface of the devices, as most of the heat is generated in a junction area in a thin layer close to the top surface of the power device (see Figure 7).

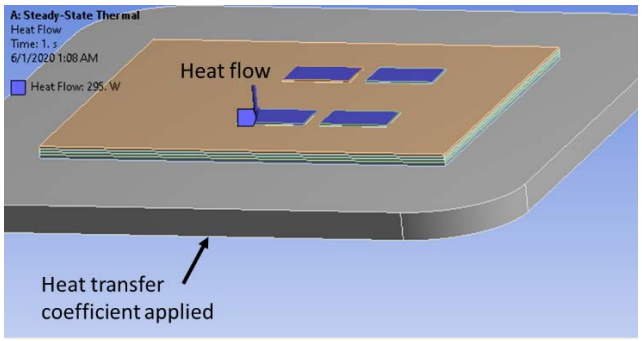

Figure 7. Heat load applied to the top surface of the power devices and the heat transfer coefficient (HTC) is applied to the bottom of the copper base plate.

Coolant temperature was assumed at $T_{fluid} = 65°C$ and the convective heat transfer coefficient (HTC) was applied to the internal surfaces of the cooling jacket and the back surface of the power module copper base plate (see Figure 8, Figure 9, and Figure 10), which is exposed to the coolant flow or impinging jets through the openings in the case enclosure. HTC was varied from $h = 20–75{,}000$ W/m^2·K for each configuration. The HTC range spans from the upper end of air natural convection (20–25 W/m^2·K), to forced air convection (50–500 W/m^2·K), to forced liquid (WEG) convection with jet impingement towards the higher end (500–50,000+ W/m^2·K) and phase-change (10,000–75,000+ W/m^2·K) cooling techniques.

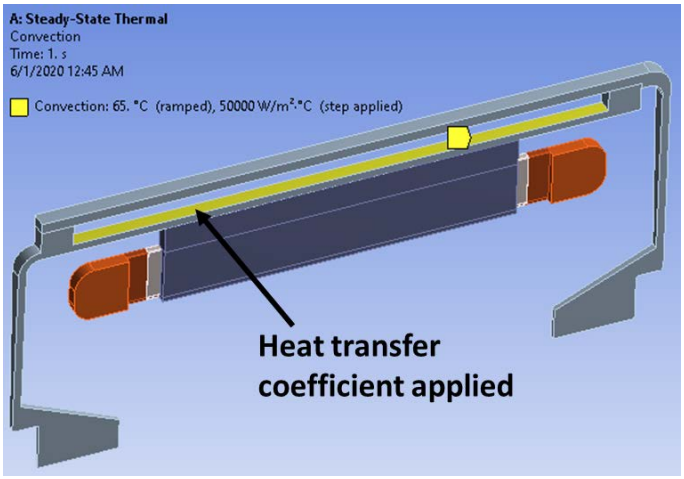

Figure 8. HTC applied to the internal surfaces of the cooling jacket—separate motor enclosure configuration shown.

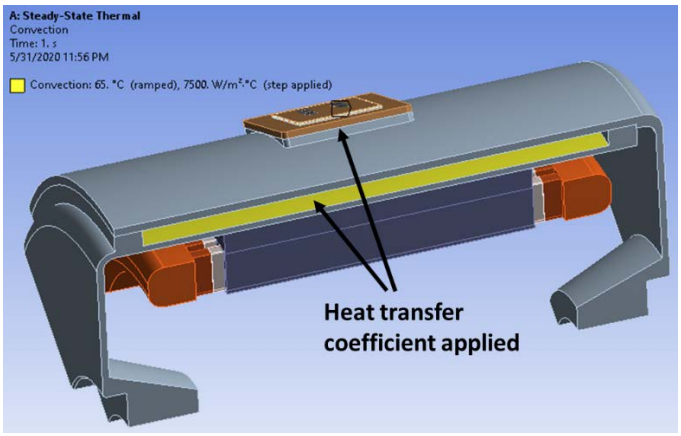

Figure 9. HTC applied to the internal surfaces of the cooling jacket and the back of the power module copper base plate—radially integrated configuration shown.

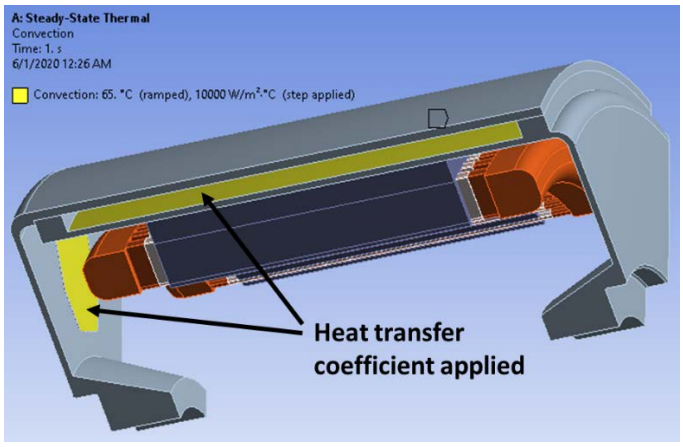

Figure 10. HTC applied to the internal surfaces of the cooling jacket and the back of the power module copper base plate—axially integrated configuration shown.

RESULTS AND ANALYSIS

FEA thermal simulations were performed for a number of HTCs, and results for the three integration configurations were compared. Temperature distributions in key components for each configuration were similar. The integrated power electronics cooling approach for both the radial and axial integration configurations seem reasonable, as the SiC power device temperatures were below key motor component temperatures. For illustration, one set of results is provided in Figure 11, Figure 12, and Figure 13. Figure 11 displays the temperature distribution in the power module, while Figure 12 and Figure 13 show the temperature distributions for a case with applied HTC of h = 10,000 W/m^2·K in the radially and axially integrated configurations, respectively. The temperature distribution in a motor with separate enclosure (Case 1) is expected to be similar to the two other integration configurations and is not shown.

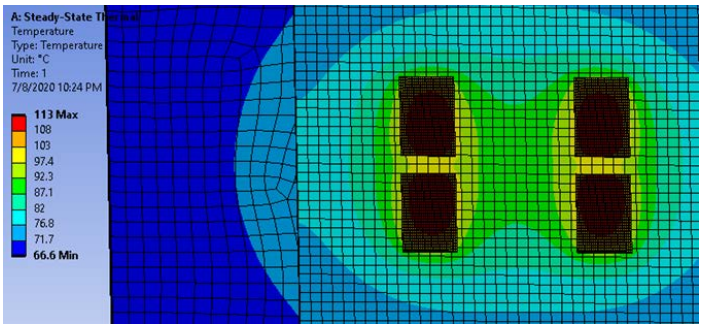

Figure 11. Temperature distribution in the FEA thermal model of a power module based on SiC devices.

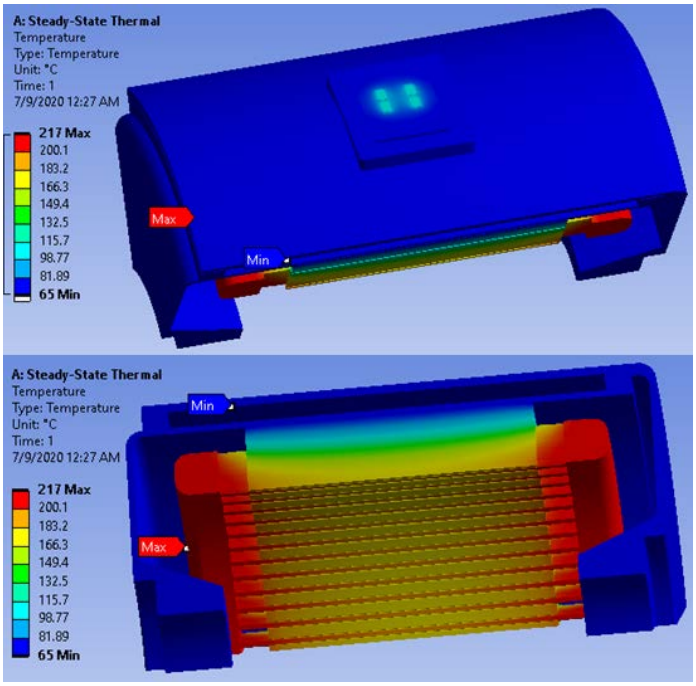

Figure 12. Temperature distribution from the FEA thermal model for the radially integrated BMW i3 motor and power module based on SiC devices (applied HTC of h = 10,000 W/m^2·K). The top image is showing a location and temperatures of the integrated power module in the motor case. The lower image is showing temperature distribution in the key motor components.

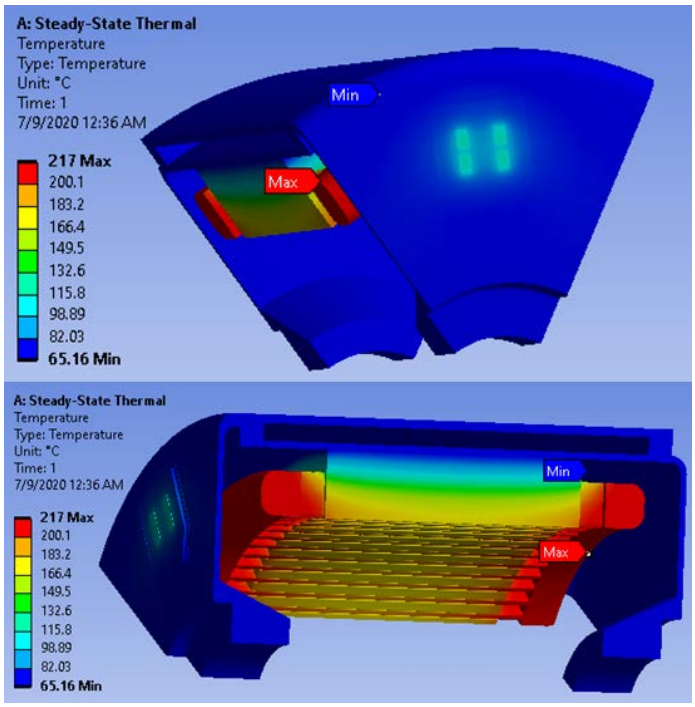

Figure 13. Temperature distribution from the FEA thermal model for the axially integrated BMW i3 motor and power module based on SiC devices (applied HTC of h = 10,000 W/m^2·K). The top image is showing a location and temperatures of the integrated power module in the motor case. The lower image is showing temperature distribution in the key motor components.

As can be seen from Figure 12 and Figure 13, the highest temperatures can be observed in the winding end-turns, where a large amount of heat is generated and the thermal path resistance to the cooling fluid is the highest. From a thermal management perspective, the application of ATF jet impingement cooling technique to winding end-turns may benefit overall temperature distributions within the traction drive. In the radial integration configuration, due to limited space in the cooling jacket channels, it may be difficult to substitute WEG coolant with ATF jet impingement for power module cooling, but the axial integration provides an excellent opportunity for cooling the back side of the power module with ATF jets. With a single delivery channel, nozzles could be positioned with jets on one side impinging on the winding end-turns, and jets in the opposite direction cooling the back side of a power module.

All three integration approaches yield volumetric and weight savings compared to the traditional traction system solutions. In the baseline case (1), simply bringing power electronics closer and attaching it to the electric motor eliminates the electric motor to power electronics interconnection harness and reduces the number of required parts. However, this minimal integration approach most likely requires either separate parallel cooling loops or single sequential coolant flow in the electric motor and the power electronics enclosures. In the radial

integration case (2), the cooling options are limited to a shared cooling jacket with circulating WEG, cooling both the electric motor and the power electronics. For the axial integration case (3), both WEG and ATF jet impingement cooling options are available. If the WEG cooling option is selected, the coolant channels can be integrated in the front/back of the motor casing, converting it to a cold plate, as well as the traditional radial cooling jacket. In case of ATF jet impingement cooling, a single channel can deliver fluid both to winding end-turns and the back of the power electronics.

CONCLUSIONS

This paper provides a comparison of the thermal management approaches for integrated traction drives. Integration of power electronics into the electric motor helps achieve higher power densities in the electric traction drive systems. The benefit of integration from the thermal management perspective is the potential for using a single-fluid loop instead of two separate cooling systems for the electric machine and the power electronics/inverter. Based on the current market and research publications overview, three main approaches were identified for integrated electric traction drives:

(1) Power electronics enclosure attached to the electric motor case, eliminating the wire harness, but with separate (often sequential) cooling paths,

(2) Power electronics radially integrated into the electric motor case with a shared cooling loop,

(3) Power electronics axially integrated into the front/back of the electric motor enclosure with potentially single-fluid cooling solution (circulating WEG or using ATF jet impingement).

All three approaches yield reasonable cooling for power electronics, with the latter approach (3) providing the option for efficient direct cooling of the motor winding end-turns, thereby reducing thermal resistance and further lowering key component temperatures.

The analysis is expected to be directly useful to researchers and motor manufacturers in the design and development of power-dense, high-performance electric machines.

ACKNOWLEDGMENTS

The authors would like to acknowledge the support provided by Susan Rogers, Technology Manager of the Electric Drive Technologies Program, U.S. Department of Energy Office of Energy Efficiency and Renewable Energy Vehicle Technologies Office. The authors would like to also acknowledge the support from Emre Gurpinar and Tsarafidy Raminosoa in Oak Ridge National Laboratory's Power Electronics and Electric Machinery Group's research and development staff.

This work was authored in part by the National Renewable Energy Laboratory, operated by the Alliance for Sustainable Energy, LLC, for the U.S. Department of Energy (DOE) under Contract No. DE-AC36-08GO28308. Funding was provided by the DOE Vehicle Technologies Office Electric Drive Technologies Program. The views expressed in the article do not necessarily represent the views of the DOE or the U.S. Government. The U.S. Government retains and the publisher, by accepting the article for publication, acknowledges that the U.S. Government retains a nonexclusive, paid-up, irrevocable, worldwide license to publish or reproduce the published form of this work, or allow others to do so, for U.S. Government purposes.

REFERENCES

[1] Hendershot, J. R. and Miller, T. J. E., 1994, "Design of brushless permanent-magnet motors." Magna Physics Pub., Oxford, UK.

[2] Bennion, K. and Cousineau, J., 2012, "Sensitivity analysis of traction drive motor cooling," *IEEE Transportation Electrification Conference and Expo (ITEC)*, pp. 1–6.

[3] U.S. DRIVE, 2017, "Electrical and Electronics Technical Team Roadmap." https://www.energy.gov/sites/prod/files/2017/11/f39/EETT%20Roadmap%2010-27-17.pdf.

[4] Bosch, "The modular eAxle drive system." https://www.bosch-mobility-solutions.com/en/products-and-services/passenger-cars-and-light-commercial-vehicles/powertrain-systems/electric-drive/eaxle/.

[5] Krivevski, B., 2019, "Vitesco Technologies Supplies Electric Drive for New Volume-Production Models of Groupe PSA and Hyundai." *Electric Cars Report*, October 16, 2019. https://electriccarsreport.com/2019/10/vitesco-technologies-supplies-electric-drive-for-new-volume-production-models-of-groupe-psa-and-hyundai/.

[6] Kane, M., 2014. "Siemens Integrates Electric Car Motor/Inverter Into Single Unit. *Inside EVs*, November 15, 2014. https://insideevs.com/news/323281/siemens-integrates-electric-car-motor-inverter-into-single-unit/.

[7] Tenconi, A., Profumo, F., Bauer, S.E. and Hennen, M. D., 2008, "Temperatures Evaluation in an Integrated Motor Drive for Traction Applications," *IEEE Transactions on Industrial Electronics*, Vol. 55, No. 10, pp. 4800–4805.

[8] Ullah, S., Winterborne, D. and Lambert, S. M., 2019, "Next-Generation Integrated Drive: A High Power Density Permanent Magnet Synchronous Drive with Flooded Stator Cooling." *J. Eng.*, Vol. 2019, Iss. 17, pp. 4231–4235.

[9] Wang, J., Li, Y. and Han, Y., 2015, "Integrated Modular Motor Drive Design With GaN Power FETs", *IEEE Transactions on Industry Applications*, Vol. 51, No. 4, July–August 2015.

[10] Chowdhury, S., Gurpinar, E., Su, G., Raminosoa, T., Burress, T. A. and Ozpineci, B., 2019, "Enabling Technologies for Compact Integrated Electric Drives for Automotive Traction Applications," *2019 IEEE Transportation Electrification Conference and Expo*

(ITEC), Detroit, MI, pp. 1–8, doi: 10.1109/ITEC.2019.8790594.

[11] Burress, T., 2016, "Benchmarking EV and HEV Technologies," [Online]. Available: https://www.energy.gov/sites/prod/files/2016/06/f32/edt006_burress_2016_o_web.pdf, Accessed July 7, 2020.

[12] Burress, T., 2017, "Electrical Performance, Reliability Analysis, and Characterization," [Online]. Available: https://www.energy.gov/sites/prod/files/2017/06/f34/edt087_burress_2017_o.pdf, Accessed July 7, 2020.

[13] Gurpinar, E. and Ozpineci, B., 2018, "Loss Analysis and Mapping of a SiC MOSFET Based Segmented Two-Level Three-Phase Inverter for EV Traction Systems," *2018 IEEE Transportation Electrification Conference and Expo (ITEC)*, Long Beach, CA, pp. 1046–1053, doi: 10.1109/ITEC.2018.8450188.

[14] Su, G. and Tang, L., 2012, "A segmented traction drive system with a small dc bus capacitor," *2012 IEEE Energy Conversion Congress and Exposition (ECCE)*, Raleigh, NC, pp. 2847–2853, doi: 10.1109/ECCE.2012.6342375.